Characterization and Optimal Design of a new Double Sampling *c* Chart

Manuel Campuzano (Universitat de Valencia),
Andrés Carrión (Universitat Politecnica de Valencia),
Jaime Mosquera (Universidad del Valle)

Abstract: In statistical process control, the Shewhart c chart is the most used tool to monitor the mean number of nonconformities. This chart is easy to use but its ability to detect small shifts in the process is low. To improve its an inspection on a larger unit is required, increasing sampling-related costs. This paper proposes a new double sampling scheme for c control chart (DS-c) that can be designed to improve the performance of c or to reduce the inspection cost. The mathematical expression required to do an exact evaluation of Average Run Length (ARL) and Average Sample Size (ASN) is deduced. Further, a bi-objective genetic algorithm is implemented to obtain the optimal design of the DS-c scheme. This optimizatión is aimed to simultaneously minimizing the error probability type II (β) and the ASN, guaranteeing a desired level for the error probability type I (α). A performance comparison between the Double Sampling (DS), Fixed Parameters (FP), Variable Sample Size (VSS) and Exponential Wigthed Moving Average (EWMA) schemes for the c control chart is carried out. The comparison shows that with the implementation of DS-c scheme is obtained a significant reduction of the out of control ARL (ARL_1) with a lower ASN respect to FP scheme and a better ARL profile than VSS scheme.

Keywords: Statistical Process Control; Number of nonconformities; c Chart; Double Sampling; Optimal Design.

1 Introduction

The conventional Shewhart c control chart is the statistical tool frequently used for monitoring the mean number of nonconformities. According to Montgomery (2009) the number of opportunities or potential locations for nonconformities is infinitely large and the probability of occurrence of a nonconformity at any location of an inspection unit is small and constant. Consequently, c chart is based on the assumption that the occurrence of nonconformities on an inspection unit is well modeled by a Poisson distribution. The inspection unit may be a single unit of product or a collection of units, when the output of process is a single unit. When the output of process is a continuous unit, the inspection unit is made up of a fraction of the product whose size is predetermined.

To monitor the process, an inspection unit, with fixed and predefined size and interval time, is drawn from the process and the observed number of nonconformities is plotted. A point plotting out-side the intervals between preset control limits is interpreted as an out of control signal.

The ability of classic c chart to detect small-to-moderate shifts in the mean number of nonconformities is low. A greater inspection units is required to improve its performance, increasing sampling-related costs. Over the last decades, different proposals have been developed in order to improve the performance of classical Shewhart control charts, and *c* control chart has not been an exception. Many of these proposals have been oriented to allow the variation on time of one or more design parameters of the control chart, such as sample size or sampling interval. Among these schemes are the Variable Sample Size (VSS), Variable Sampling Interval (VSI) and Variable Sample Size and Interval (VSSI). These adaptive schemes have been shown to be more effective than Fixed Parameter (FP) schemes to detect small-to-moderate shifts in the process. A review of recent developments in design of adaptive control charts has been elaborated by Psarakis (2015).

Adaptive control charts for attributes were initially proposed by Vaughan (1992), who proposed a VSI scheme for *np* control chart. Years later Epprecht and Costa (2001) and Epprecht et al. (2003) developed and optimized a VSS scheme for *np* and *c* control charts. Later, Wu and Luo (2004) worked in order to optimize these adaptive control charts. Furthermore to the classic Shewhart control charts, authors have also investigated the development of adaptive control scheme applied to EWMA control charts. Epprecht et al. (2010) developed a VSI scheme for EWMA-*c* control charts, obtaining optimal designs for this chart as well as for the fixed sampling interval.

Double Sampling (DS) is another alternative that has been considered to improve the performance of control charts. The first ideas about DS schemes were introduced by Croasdale (1974). He proposed a DS scheme for the $\overline{X}$ control chart, used to monitoring a quantitative variable. In this scheme two samples are drawn from the process. The information collected from the first sample is used to decide whether process is in-control state or if the analysis of second sample is required. The out of control state of process is diagnosed using only information from the second sample. Later, Daudin (1992) proposes to use the joint information of first and second samples for diagnosis of the out of control state and considers the possibility that the out of control signal will be generated in the first sample. This procedure improves the performance of Croasdale's DS. The design parameters of Daudin's DS was optimized to minimize Average Sample Number (ASN). Instead of minimizing ASN, Irianto and Shinozaki (1998) proposes to maximize the power $(1-\beta)$ of the DS-$\overline{X}$ control chart.

Subsequently, these ideas about DS schemes was implemented for attribute control charts. De Araújo Rodrigues et al. (2011) proposed a DS-*np* control chart, developed to improve the performance of traditional *np* chart. This scheme is deployed in two stages. On the first stage, the first sample fraction is inspected and analyzed, depending on the results, a final decision is made or it goes on to second stage, where remaining sample fractions are inspected. Afterwards, the joint information of first and second stage is used to diagnose the process. Similarly, Perez et al. (2010) proposed the DS-*u* scheme. The design of DS-*u* chart was optimized to maximize the power $(1-\beta)$ of the control chart, using a genetic algorithm.

Some additional innovations for the DS scheme have been implemented. Wu and Wang (2007) proposes a modified DS scheme for the *np* control chart. In this scheme, the first subsamples is used only to diagnose the in-control state of the process or to decide if it is required to analyze the second subsample. When the second sample is required, the diagnosis of the out of control state is performed using the location of the first non-conforming unit observed on second sample. With this scheme a false alarm rate closer to target and a better performance in detection of the shift are obtained. Recently

Chong et al. (2014) developed a synthetic DS *np*. This chart uses the DS-*np* proposes by De Araújo Rodrigues et al. (2011) and it is complemented with a control chart for Conforming Run Length (Number of units observed until the first nonconforming). With this scheme, a faster detection of shift is obtained, compared to those observed for the synthetic *np* and DS-*np* schemes.

This paper aims to propose a new DS scheme for *c* control chart. As it will be shown, the new DS-*c* scheme offers better statistical efficiency than the classical FP-*c* charts without increased sampling cost. Alternatively, the scheme can be used to reduce the sampling cost without reducing the statistical efficiency. Recently a similar, but not equal, scheme was proposed by Inghilleri et al. (2015), who designed a DS-*c*. Their proposal is supported on an approximation to normal distribution, which is adequate only for very large inspection unit. In contrast, our proposal is supported on the exact probability distribution for the number of nonconformities and a bi-objective optimization approach is implemented.

The paper is organized as follows. After this introductory section, Section 2 shows a description of proposed DS-*c* scheme and its decisions rules for the process diagnosis. In Section 3, the performance measures for DS-C control scheme are obtained. In Section 4, a bi-objective optimization is carried-out to obtain the optimal parameters of DS-*c* scheme and an illustrative example is shown. Section 5 contains a comparison of efficiency of DS-*c* chart versus the alternatives with fixed parameter (FP-*c*), VSS-*c* and EWMA-*c*. Finally, Section 6 summarizes the conclusions of the paper.

2 The DS-*c* chart.

Let us suppose a process for which the observed number of nonconformities, on an standard inspection unit of size (k), follows a Poisson distribution with mean λ. While the process remains in-control state, the mean number of non-conformities is $\lambda = \lambda_0$. If an assignable cause is present, implying that process is becoming lower quality, there is an increase on mean number of non-conformities to level $\lambda = \lambda_1$ $(\lambda_1 > \lambda_0)$. Only this shift is considered of interest, therefore the chart is defined without lower control limit.

The proposed DS-*c* scheme has five design parameters: The fraction (m_1) for the first sub-sample; The acceptance number for the first stage, corresponding to a warning limit (WL); The rejection number for the first stage (UCL_1); The fraction (m_2) for the second sub-sample; and the acceptance number for the second stage (UCL_2).

Once the design parameters are predefined, the following procedure is proposed to monitor the process:

1. A global sample of size $(m_1 + m_2) * k$ is drawn from process.

2. A first sample fraction of size $m_1 * k$ is analyzed, searching for non-conformities. Let x_1 denote the observed number of nonconformities in this sub-sample. In this case the decision depends on x_1:

   A. If $x_1 < WL$, the process is considered in-control and the control scheme continues operating.

B. If $x_1 > UCL_1$, the process is supposed to be out of control and a corrective action should be taken.

In either case (A or B), the second sub-sample does not need to be analyzed.

3. If $WL < x_1 < UCL_1$, the second sample fraction of size $m_2 * k$ is analyzed, searching for non-conformities. Let x_2 denote the observed number of nonconformities in this sub-sample. In this case the decision depends on sum of x_1 and x_2:

C. If $(x_1 + x_2) < UCL_2$, the process is considered in control and the control scheme continues operating.

D. If $(x_1 + x_2) > UCL_2$, the process is considered out of control and a corrective action should be taken.

4. At prefixed sampling intervals (every hour, for example), return to first stage and draw a new global sample of size $(m_1 + m_2) * k$.

To avoid confusion in decision rules, we recommend that locations of the limits WL, UCL_1 and UCL_2 do not match with any integer number. Instead, we suggest locating them in midpoint of two consecutive integers. Figure 1 shows the graphical appearance for DS-c scheme. The points are plotted according to situations A, B, C and D, above described.

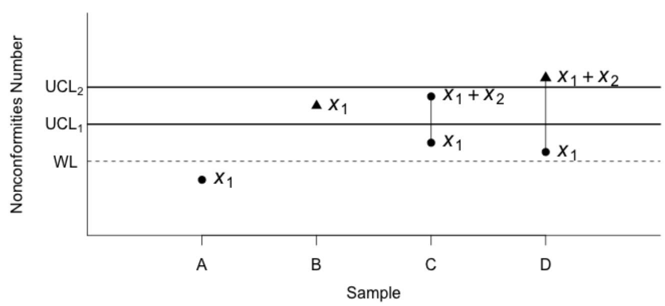

Figure 1: DS-c graphical appearance.

As defined in the operation rule of DS-Scheme, the two sub-samples come from the same global sample, therefore there is a guarantee that they come from the same distribution. Also it is assumed that global samples are independent.

3 Performance measures.

In Statistical Process Control, the efficacy of a control chart is usually determined by its ability to detect a shift in the process. This ability is measured by the probability of issuing an alarm (Pa) or by the Average Run Length (ARL), which represents the average number of points that are plotted until an alarm is signaled. If samples are independents, ARL is inverse to Pa.

$$ARL = \frac{1}{Pa}. \tag{1}$$

Specifically for the DS-*c* scheme, Pa depends on the set of design parameters $(m_1, m_2, WL, UCL_1, UCL_2)$ and on mean number of nonconformities per inspection unit (λ):

$$\begin{aligned} Pa &= 1 - P\{(x_1 < WL|\lambda) \cup ((WL < x_1 < UCL_1|\lambda) \cap (x_1 + x_2 < UCL_2|\lambda))\} \\ &= 1 - P(x_1 < WL|\lambda) + \sum_{i=\lceil WL \rceil}^{\lfloor UCL_1 \rfloor} P(x_1 = i|\lambda) * P(x_2 < UCL_2 - i|\lambda), \end{aligned} \tag{2}$$

Where:

$$P(x_1|\lambda) = \frac{e^{-\lambda m_1} * (\lambda m_1)^{x_1}}{x_1!}, \tag{3}$$

$$P(x_2|\lambda) = \frac{e^{-\lambda m_2} * (\lambda m_2)^{x_2}}{x_2!}. \tag{4}$$

If Pa is evaluated for the in-control state of process ($\lambda = \lambda_0$), the probability of false alarm (α) is obtained. In this case, $ARL = 1/\alpha$ is denoted as ARL_0 (In-control ARL). Conversely, if Pa is evaluated for the out of control state of process ($\lambda = \lambda_1$), the probability of detect the shift ($1 - \beta$) is obtained. Generally ($1 - \beta$) is named as test power. In this case, $ARL = 1/(1 - \beta)$ is denoted as ARL_1 (Out of control ARL).

The Average Sample Number (ASN) is another attractive indicator that should be considered in performance evaluation of adaptive sample size schemes. The ASN is directly related to inspection cost and can be used as an input to evaluate it. In the context of DS-*c* scheme, the ASN measures the average fraction, of a standard inspection unit of size (k), which will be analyzed. The ASN is a function of λ, of the sample fractions (m_1, m_2) and the control limits of first stage (WL, UCL_1):

$$ASN = m_1 + m_2 * P(WL < x_1 < UCL_1|\lambda). \tag{5}$$

Where $P(WL < x_1 < UCL_1|\lambda)$ is the probability of going to second stage. According to current notation, ASN_0 is the in-control ASN and ASN_1 is the out of control ASN.

Note that performance indicators (Pa, ARL, ASN) do not depend on size of the standard inspection unit (k). This is due to that, in DS-*c* scheme, the standard inspection unit is only the dimension reference on which the in-control mean number of nonconformities (λ_0) is established. In practice, the real inspection units will have a size $m_1 * k$, in first stage, and $m_2 * k$, in second stage. The effect of modifying the size of inspection unit is picked up by the proportional adjustment of λ. This implies that, without loss of generality, the performance evaluation can be done assuming that standard inspection unit is a reference unit with relative size $k = 1$.

4 Optimal design of the DS-*c* scheme.

Optimizing the performance of DS-c scheme is equivalent to finding the setting of design parameters that guarantee that, during monitoring, the chart will have: 1. A tolerable probability of false alarm; 2. A good performance to detect a critical increment in the mean number of nonconformities per unit ($\lambda_1 = \gamma^* \lambda_0$), and 3. Reduced inspection costs.

The tolerable value for the probability of false alarm (α^*) and the critical magnitude of shift for the process (γ^*) should be prefixed by practitioner. In addition, he should evaluate the technical and economical constrains for the sampling procedure. For example, the practitioner should establish the smallest and largest inspection unit that can be manipulated in each sampling stage. These references may be used to restrict the search range of fraction m_1 over interval ($m_1.min$; $m_1.max$) and fraction m_2 over interval ($m_2.min$; $m_2.max$).

Once these references are established. The problem is considered as a bi-objective optimization problem, in which:

Given: $(\alpha^*, \lambda_0, \gamma*, m_1.min, m_1.max, m_1.min, m_2.max)$.

Find: $(m_1, m_2, WL, UCL_1, UCL_2)$.

That minimize:

$$min : Z_1 = \beta \quad \text{equivalent to} \quad min : Z_1 = ARL_1, \tag{6}$$
$$min : Z_2 = ASN_0. \tag{7}$$

Subject to:

Desired probability of false alarm

$$\alpha \leq \alpha^*, \tag{8}$$
$$\tag{9}$$

Location of control limits

$$WL \geq 0.5, \tag{10}$$
$$UCL_1 - WL \geq 1, \tag{11}$$
$$UCL_2 - UCL_1 \geq 0 \tag{12}$$

Size of subsamples

$$m_1.min \leq m_1 \leq m_1.max, \tag{13}$$
$$m_1 \leq m_2, \tag{14}$$
$$m_2 \leq m_2.max. \tag{15}$$

The above problem relate two contradictory objectives (*Minimizing* β, *Minimizing* ASN_0). This mean that is a competition between the objectives, therefore the optimal solution for β is not the optimal solution for ASN_0. To solve the problem, some criteria must be defined in order to determine which solutions are considered good quality and which are not. In these sense Zitzler and Thiele (1999) introduces the concept of dominance, which it is useful to classify the solutions of a multi-objective problem.

For each of M objectives, the operator $\lhd$ between two solutions (p_i, p_i') $(f_j(p_i) \lhd f_j(p_i'))$ indicates that p_i is better than p_i' for the particular objective j, likewise $(f_j(p_i) \rhd f_j(p_i'))$ indicates that p_i is worse than p_i' for the particular objective j. It will be affirmed that p_i dominate p_i' if only if following conditions are met:

- p_i is not worse than p_i' with respect to all objectives; $f_j(p_i) \not\rhd f_j(p_i')$, for all $j \in 1, 2, 3, ..., M$
- The solution p_i is much better than p_i' in at least one objective; $f_j(p_i) \lhd f_j(p_i')$ in at least one $j \in 1, 2, 3, ..., M$

Therefore, p_i dominates to p_i' or p_i' is dominated by p_i.

If it is found that the first condition of dominance is not fulfilled for either of the two solutions, it is not possible to conclude about the dominance of one with respect to another. When this happens, it is said that the solutions are un-dominated. In this way, if one has a finite set of solutions P and a comparison of all possible pairs is made, in the end one will have a subset of solutions P' that are not dominated by each other and this set has the property of dominating the rest of solutions that do not belong to it. This subset P' is called the Pareto front. When the set P is the search space, P' is called the Pareto optimal front Zitzler and Thiele (1999). A procedure to obtain the Pareto optimal front is summarize below.

1. Make $i = 1$.
2. For all $i' \neq i$, compare the solutions p_i and p_i' to determine dominance.
3. If for some i', p_i is dominated by p_i', mark p_i as dominated. Increase i by one and go to step 2.
4. If all solutions (that is, when $i = N$ is reached) in the set P was considered, go to step 5.
5. All solutions that are not marked as dominated are non-dominated solutions.

Note that in order to obtain the exact Pareto optimal front, the comparison between all pairs of feasible solution has to be done. However, in many cases, as in the DS-*c* optimization problem, the search space is too large and the comparison is computationally expensive. Another alternative consists in have an exact mechanism to generate the subset of non-dominated solutions. From equations (1 to 5) it can be deduced that the mathematical expression to calculate the performance indicators (α, β, ASN) do not correspond to linear functions, whereby using analytic and exact solving tools for generate the subset P' is not possible, at least from our knowledge. For this reason we proposed the implementation of a multiobjective Genetic Algorithm.

Genetic algorithms, introduced by Holland (1975), are a family of computational models inspired by evolution. These algorithms encode a potential solution to a specific problem on a simple chromosome like data structure, and apply recombination operators to these structures in such a way as to preserve critical information. Whitley (1994). The Genetic Algorithms have been widely used by different authors as a tool to optimize control charts, recognized work in the area as: He et al. (2002), Aparisi and Garcia-Diaz (2004), Chou et al. (2006) and recently Aparisi et al. (2018).

The Nondominated Sorting Genetic Algorithm (NSGA-II), developed by Deb et al. (2002), is an excellent option for multi-objective optimization, since it is classified as elitist because it incorporates a mechanism of preservation of the dominant solutions through several generations of a genetic algorithm. In NSGA-II, the process starts with a set of parent solutions P_t of size N, that is obtained at random or through a soft construction. The following generations are determined using modified crossing and mutation selection mechanisms defined by the classical genetic algorithm. The descendant population Q_t (size N) is created using the parent population P_t (size N). Later on, the two populations are combined to form $R_t = P_t \cup Q_t$ of size $2N$. After the above, by means of a non dominated order, R_t is classified in different fronts of Pareto. Although this requires more effort, it is justified by allowing a global verification of dominance between the population of parents and descendants. Once the ordering process has finished, the new population is generated from the sets of the non-dominated fronts. This new population begins to be built with the best front that has not been dominated (F_1), continues with the solutions of the second front (F_2), third (F_3). Since the population R_t is of size $2N$, and only N should to make up the descendant population, not all the set of fronts belonging to the population R_t can be accommodated in the new population. Those fronts that can not be accommodated disappear.

The NSGA II algorithm is available in R Statistical Software through the package **mco**, developed by Mersmann et al. (2014). This package was used as a tool to solve the bi-objective optimization problem of design of DS-*c* scheme and obtain the Pareto front. To illustrate the optimization procedure and the operation of the DS-*c* scheme, an application example is developed in section 4.1

4.1 Application Example

In a textile finishing plant, the dyed fabric is inspected to verify the presence of defects. In inspection, a sample of $k = 9mts^2$ of cloth is drawn and the observed number of defects is counted. In regular operating conditions (in-control) the process presents a mean of $\lambda_0 = 0.5$ defects per inspection unit. An increase in the mean number of defects at the level $\lambda_1 = 1.0$ ($\gamma^* = 2.0$) is critical for this process.

Currently, the process is monitored with an FP-*c* scheme with upper control limit located in $UCL = 3.0$. This FP-*c* scheme has a false alarm probability of $\alpha = 0.00175$ ($ARL_0 = 570.9$) and probability to detect the critical shift of $1 - \beta = 0.0189$ ($ARL_1 = 52.66$). As an alternative to reduce the detection time of critical shift, without increasing the probability of false alarm, the implementation of a DS-*c* scheme with optimal design is considered.

Due to operational restrictions in process, the largest inspection unit that can be drawn is 45 mts^2 ($m_2.max = 5.0$) and smallest of 1.8 mts^2 ($m_1.min = 0.2$). To these restrictions, a restriction on the probability of false alarm desired for the DS-C scheme is added ($\alpha \leq 0.00175$). When the optimization algorithm runs, the Pareto front shown in Figure 2 is obtained.

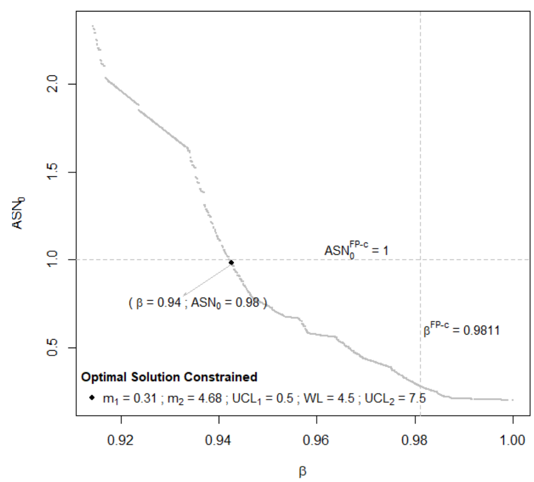

Figure 2: Pareto front for the illustrative example.

In Figure 2, the horizontal and vertical dotted lines indicate the performance reference of FP-*c* scheme, currently used. Those solutions located between pair of reference lines correspond to settings of DS-*c* schemes under which an improvement is obtained in both performance criteria (β, ASN_0). To select the optimal solution, the practitioner must establish a trade off between the improvement in speed of shift detection and reduction of inspection costs. For this example case, given that economical resource to cover the inspection costs is currently available, the solution with the best performance in detecting the shift (minimum β), without incurring an additional cost ($ASN_0 \leq 1.0$) is chosen. According to this criterion, the optimal design is the setting ($m_1 = 0.31, m_2 = 4.68, WL = 0.5, UCL_1 = 4.5, UCL_2 = 7.5$). Table 1 shows a comparison of performance indicators ($ARL_0(\alpha), ARL_1(\beta), ASN_0$) for the FP-*c* and DS-*c* schemes.

Table 1 Performance summary of FP-*c* and Optimal DS-*c* for illustrative example.

Scheme	$ARL_0 - (\alpha)$	$ARL_1 - (\beta)$	$ASN_0 - (mts^2)$
FP-*c*	570.9 - (0.00175)	52.66 - (0.981)	1.00 - (9.00)
DS-*c*	571.1 - (0.00175)	17.42 - (0.943)	0.98 - (8.84)

The summary shows that optimal DS-*c* scheme will have a better performance (lower ARL_1) in detection of critical shift. On average, the DS-*c* scheme will use 17.42 samples to detect the shift, while FP-*c* scheme will average 52,66 samples. If we assume that both schemes use the same sampling frequency, this is equivalent to reducing in 66.92% the mean time of detection of shift. Additionally, both the false alarm rate and inspection costs are practically the same as those currently presented by FP-*c* scheme. According to optimal design, in inspection a sample of $9 * (0.31 + 4.68) = 44.91\ mts^2$ is drawn. Initially, only an area of $9 * (0.31) = 2.79\ mts^2$ is inspected and plotted x_1: the number of defects over the first subsample. Only if $1.5 \leq x_1 \leq 4.5$ will it be necessary to check the remaining $42.12\ mts^2$.

To illustrate the differences in the operation of FP-*c* and DS-*c* schemes, the inspection of the process has been simulated. In both cases, the first 10 samples were simulated under in-control state ($\lambda = 0.5$). From sample 11, the process was simulated under out-of-control state ($\lambda = 1.0$). Figure 3 shows the result obtained by carrying the FP-*c* and DS-*c* control charts for simulated samples.

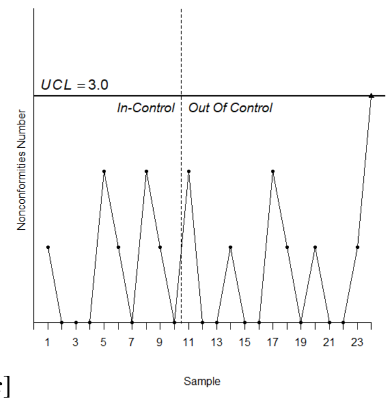

[FP-*c*]

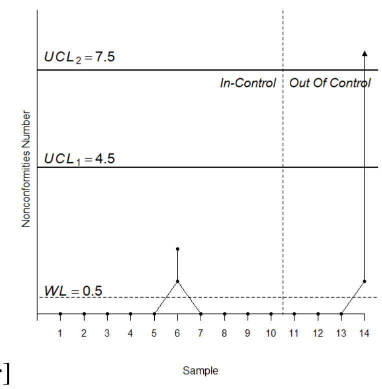

[DS-*c*]

Figure 3: Simulation of operation of the a) FP-*c* and b) Optimal DS-*c* for the illustrative example.

As can be observed, when control was performed with FP-*c* scheme, the shift is detected in sample 24, 14 samples after the occurrence of shift. With DS-*c* scheme the signal is presented earlier, in sample 14, only 4 samples after that shift in process occurs. Note that in DS-*c* scheme, only two samples (6 and 14) required verification of all global sample. In remaining 12 samples, the in-control diagnosis was made with inspection of only the first subsample.

For this particular example, the implementation of DS-*c* scheme leads to greater efficiency in process monitoring. A wider comparison of performance of DS-*c* scheme, which includes other control schemes, is presented in Section 5.

5 Comparative evaluation of the performance of DS-*c* scheme.

In this section a broad performance evaluation of optimal DS-*c* scheme is carried out, in order to quantify the benefit that its application may have in contrast as to the use of a traditional FP-*c* scheme. To have a wider reference, optimal VSS-*c* scheme, proposed by Epprecht et al. (2003), and optimal EWMA-*c* chart by Borror et al. (1998) and used by Epprecht et al. (2010), are included in comparison. As it was shown in section 3, without loss of generality, the performance evaluation is made taking as reference a standard unit of inspection of size $k = 1$.

To make a fair comparison between four alternative schemes, it is necessary to ensure that its designs are obtained under similar conditions and restrictions. For example, the four schemes must have similar inspection costs and false alarm rates. As mentioned in section 3, The inspection costs depends directly on size of the inspection unit. In FP-*c* and EWMA-*c* schemes, the size of the inspection unit is always the same (k) and the inspection cost also will be constant. In contrast, in VSS-*c* and DS-*c* schemes the sample size varies between two quantities and the inspection cost is variable. However, it is still possible to guarantee the similarity of the inspection cost of the four schemes. For this purpose, the design constrain $ASN_0 \leq 1$ is include in the optimization procedure of VSS-*c*. On the other hand, the optimization procedure of DS-*c* generates a Pareto front. From this Pareto, those optimal solution that satisfies the condition $ASN_0 \leq 1$, with a lower β value is chosen (as in illustrative example). It will be the solution with the best out of control performance and same or inferior inspection cost that FP-*c* and EWMA-*c* schemes.

Also it is know that, due to its discrete nature, FP-*c* scheme has limited possible value for probability of false alarm (α), which depend on value of λ_0 and location of the upper control limit (UCL). Instead, DS-*c*, VSS-*c* and EWMA-*c* schemes have a greater number of design parameters, whereby they are more flexible to meet with a desired probability of false alarm (α^*). To match the probability of false alarms of the four schemes, as much as possible, the following strategy is used:

- The usual $\alpha' = 0.00027$ ($ARL_0 = 370.42$) is used as the nominal design reference of FP-*c* scheme.
- The FP-*c* scheme with α closest to α' is selected and the real probability of false alarm (α^*) is calculated.
- α^* is used as design reference for VSS-*c*, EWMA-*c* and DS-*c* schemes.

Finally, in the design of VSS-*c* and DS-*c* the constraints on the range of variation of the fraction sample sizes $(0.2 \leq m_1 \leq 0.8)$ and $m_2 \leq 5.0$ are imposed. This restrictions are the same employed by Epprecht et al. (2003).

Once the equivalence between four schemes is guaranteed, the comparison focuses on evaluating its performance in detecting a shift of critical relative magnitude γ^*, on the mean number of non-conformities ($\lambda_1^* = \gamma^* \lambda_0$). The values considered for input parameters were as follows: $\lambda_0 = 0.5, 1.0, 1.5, 2.0, 3.0, 4.0; \gamma^* = 1.5, 2.0, 3.0$. Table 2 shows the optimal design parameters for FP-*c*, VSS-*c*, EWMA-*c* and DS-*c* schemes , under λ_0 and γ^* inputs and the corresponding ARL_0 and ARL_1. The indicator $\%ARL_1$, which is included in column 13 of Table 2, evaluates the percentage reduction of ARL_1 obtained when DS-*c* scheme is used instead of some of the alternatives schemes (Alt = FP, VSS, EWMA). This indicator is calculated as seen in equation 16.

$$\%ARL_1(Alt, DS-c) = \frac{ARL_1(Alt) - ARL_1(DS-c)}{ARL_1(Alt)} * 100\% \qquad (16)$$

Table 2: Performance and design parameters of FP-c control chart and equivalent optimal VSS-c, EWMA-c, DS-c schemes for given λ_0 and γ^*.

λ_0	γ^*	Scheme	m_1	m_2	r	WL_1	UCL_1	WL_2	UCL_2	ARL_0	ARL_1	$\%ARL_1$
0.5		FP	1				3.5		3.5	570.9	137.13	53.73
	1.5	VSS	0.54	3.64		1.5	4.5	0.5	5.5	615.5	48.53	-30.74
		EWMA	1		0.04		0.75			601.6	42.08[1]	-50.78
		DS	0.31	4.68		0.5	4.5		7.5	575.1	63.45	
		FP	1				3.5		3.5	570.9	52.66	66.93
	2.0	VSS	0.26	4.6		0.5	3.5	2.5	6.5	628.2	12.99[1]	-34.10
		EWMA	1		0.07		0.88			592.6	17.45	0.16
		DS	0.31	4.68		0.5	4.5		7.5	575.1	17.42	
		FP	1				3.5		3.5	570.9	15.23	70.06
	3.0	VSS	0.33	4.6		0.5	3.5	3.5	6.5	682.9	4.47[1]	-2.01
		EWMA	1		0.15		1.15			571.3	7.14	36.15
		DS	0.31	4.68		0.5	4.5		7.5	575.1	4.56	
1.0		FP	1				4.5		4.5	273.2	53.83	59.90
	1.5	VSS	0.38	3.08		1.5	3.5	1.5	7.5	282.3	21,77	0.82
		EWMA	1		0.06		1.39			277.1	20.40[1]	-5.8
		DS	0.52	4.96		1.5	5.5		11.5	273.8	21.59	
		FP	1				4.5		4.5	273.2	18.99	67.59
	2.0	VSS	0.21	4.19		0.5	2.5	5.5	9.5	312.2	6,62	6.95
		EWMA	1		0.16		1.82			276.6	8.77	29.81
		DS	0.52	4.96		1.5	5.5		11.5	273.8	6.16[1]	
		FP	1				4.5		4.5	273.2	5.41	58.72
	3.0	VSS	0.31	3.08		0.5	3.5	4.5	7.5	277.5	2.74	18.61
		EWMA	1		0.24		2.09			277.2	3.75	40.38
		DS	0.59	3.37		1.5	5.5		9.5	273.6	2.23[1]	
1.5		FP	1				5.5		5.5	224,4	36.54	61.26
	1.5	VSS	0.38	3.01		1.5	4.5	3.5	9.5	231.6	13.52[1]	-4.73
		EWMA	1		0.09		2.11			232.0	14.88	4.84
		DS	0.40	4.73		1.5	7.5		14.5	224.6	14.16	
		FP	1				5,5		5.5	224.4	11.92	64.66
	2.0	VSS	0.27	2.97		0.5	5.5	5.5	9.5	224.5	4.15[1]	-1.45
		EWMA	1		0.21		2.65			229.3	6.29	33.10
		DS	0.40	4.73		1.5	7.5		14.5	224.6	4.21	
		FP	1				5.5		5.5	224.4	2.87	49.46
	3.0	VSS	0.54	2.97		1.5	4.5	6.5	9.5	234.8	1.71	0.58
		EWMA	1		0.26		2.83			224.6	2.76	38.45
		DS	0.53	2.50		1.5	6.5		10.5	228.0	1.70[1]	
2.0		FP	1				6.5		6.5	220.6	29.84	64.59
	1.5	VSS	0.28	3.32		1.5	4.5	5.5	12.5	221.1	10.20[1]	-3.63
		EWMA	1		0.10		2.74			221.5	12.15	13.00
		DS	0.54	4.81		2.5	7.5		18.5	221.8	10.57	
		FP	1				6.5		6.5	220.6	9.04	63.81
	2.0	VSS	0.39	3.64		1.5	4.5	9.5	13.5	237.7	3.67	10.90
		EWMA	1		0.26		3.52			222.0	5.12	36.18
		DS	0.55	4.39		2.5	11.5		17.5	220.9	3.27[1]	
		FP	1				6.5		6.5	220.6	2.54	44.26
	3.0	VSS	0.69	2.83		2.5	5.5	9.5	11.5	224.9	1.93	26.43
		EWMA	1		0.27		3.56			228.9	2.33	39.12
		DS	0.66	2.26		2.5	8.5		12.5	224.0	1.42[1]	
3.0		FP	1				8.5		8.5	262.9	24.84	68.75
	1.5	VSS	0.39	4.88		2.5	6.5	16.5	22.5	270.3	6.70[1]	-15.82
		EWMA	1		0.16		4.32			263.5	9.85	21.19
		DS	0.55	5.00		3.5	9.5		26.5	273.6	7.76	
		FP	1				8.5		8.5	262.9	6.55	62.86
	2.0	VSS	0.48	3.72		2.5	6.5	14.5	18.5	265.8	2.89	15.91
		EWMA	1		0.25		4.80			263.1	4.01	39.43
		DS	0.60	3.54		3.5	11.5		21.5	263.4	2.43[1]	
		FP	1				8.5		8.5	262.9	1.84	35.38
	3.0	VSS	0.81	2.67		4.5	7.5	11.5	16.5	271.9	1.61	26.09
		EWMA	1		0.26		4.87			267.3	1.92	38.01
		DS	0.70	1.83		3.5	9.5		15.5	268.6	1.19[1]	

[1] Lowest ARL_1 in optimization point

Continued on next page

Table 2: Performance and design parameters of FP-*c* control chart and equivalent optimal VSS-*c*, EWMA-*c*, DS-*c* schemes for given λ_0 and γ^*. (*continued from previous page*)

λ_0	γ^*	Scheme	m_1	m_2	r	WL_1	UCL_1	WL_2	UCL_2	ARL_0	ARL_1	$\%ARL_1$
4.0		FP	1				9.5		9.5	352.1	23.46	73.31
	1.5	VSS	0.31	4.30		2.5	8.5	18.5	26.5	354.5	5.87[1]	-6.64
		EWMA	1		0.14		5.47			355.1	8.67	27.29
		DS	0.45	4.95		3.5	10.5		33.5	358.7	6.26	
		FP	1				9.5		9.5	352.1	5.43	63.21
	2.0	VSS	0.44	2.78		2.5	7.5	14.5	19.5	356.7	2.56	21.88
		EWMA	1		0.23		6.06			364.4	3.56	43.82
		DS	0.62	3.51		4.5	11.5		27.5	358.8	2.00[1]	
		FP	1				9.5		9.5	352.1	1.53	28.48
	3.0	VSS	0.84	2.20		5.5	9.5	13.5	17.5	370.9	1.44	23.61
		EWMA	1		0.23		6.06			364.4	1.77	38.01
		DS	0.72	1.61		4.5	11.5		18.5	363.7	1.10[1]	

[1] Lowest ARL_1 in optimization point

As seen in Table 2, with the implementation of the optimal DS-*c* scheme, the performance of FP-*c* control chart is remarkably improved. This happens for all pairs (λ_0,γ^*). Here, the observed reduction in ARL_1 was between (28.48%) and (73.31%) with similar inspection cost. In those scenarios with $\lambda_0 > 1.0$ and moderate to large shift magnitude ($\gamma^* = 2.0, 3.0$), the DS-*c* scheme was the best alternative, or at least very close ($\%ARL_1 > -2.0$). Only those scenarios with a very low mean number of non-conformities $\lambda_0 = 0.5$ or a small critical shift magnitude ($\gamma^* = 0.5$), one of two schemes, VSS-*c* or EWMA-*c*, has a significantly outperformance ($\%ARL_1 < -2.0$) that DS-*c* scheme.

It is common practice to optimize a control chart to obtain the best performance in detecting a specific shift magnitude. However, in a practical application, the shift magnitude for which the control chart has been optimized is only one in an infinite set of possible shifts magnitudes that the process can present. For example, in the implementation of a optimal DS-*c* scheme, the mean number of non-conformities may increase exactly in the magnitude $\gamma = \gamma^*$ for which it has been optimized, or it may present a shift of magnitude $\gamma \neq \gamma^*$ in which there is no guarantee that its performance is optimum. So as to evaluate and compare the performance of the three alternative control schemes at different shift magnitude, the ARL_1 profile evaluated for different values of γ, are presented in Table 3. Additionally, The third column of Table 3 shows the average sample size (ASN_0) required to control the process, while it is in-control state.

Table 3: ASN_0, ARL_0 and ARL_1 profile $(\gamma = 1.5 - 5.0)$ for the FP-*c* control chart and equivalent optimal VSS-*c*, EWMA-*c*, DS-*c* schemes.

					ARL_1 $\gamma = \lambda_1/\lambda_0$							
λ_0	γ^*	Scheme	ASN_0	ARL_0	1.5	2.0	2.5	3.0	3.5	4.0	4.5	5.0
0.5		FP	1.000	570.9	137.13	52.66	26.13	15.23	9.92	7.00	5.25	4.13
	1.5	VSS	0.998	615.5	**48.53**	<u>16.22</u>	9.36	6.61	5.16	4.28	3.70	3.29
		EWMA	1.00	601.6	<u>**42.08**</u>[1]	17.98	11.38	8.38	6.67	5.56	4.79	4.22
		DS	0.982	575.1	**63.45**	17.42	<u>7.73</u>	<u>4.56</u>	<u>3.22</u>	<u>2.55</u>	<u>2.17</u>	<u>1.94</u>
	2.0	VSS	0.981	628.2	50.86	<u>**12.99**</u>[1]	<u>6.59</u>	4.65	3.79	3.32	3.02	2.82
		EWMA	1.000	592.7	<u>44.75</u>	**17.45**	10.60	7.65	6.02	4.99	4.28	3.77
		DS	0.982	575.1	63.45	**17.42**	7.73	<u>4.56</u>	<u>3.22</u>	<u>2.55</u>	<u>2.17</u>	<u>1.94</u>

_ Lowest ARL_1.

[1] Lowest ARL_1 in optimization point.

Continued on next page

Table 3: ASN_0, ARL_0 and ARL_1 profile ($\gamma = 1.5 - 5.0$) for the FP-c control chart and equivalent optimal VSS-c, EWMA-c, DS-c schemes. (*Continued*)

					ARL_1							
					$\gamma = \lambda_1/\lambda_0$							
λ_0	γ^*	Scheme	ASN_0	ARL_0	1.5	2.0	2.5	3.0	3.5	4.0	4.5	5.0
	3.0	VSS	0.998	682.9	61.90	15.11	6.86	**4.47**[1]	3.51	3.03	2.75	2.56
		EWMA	1.00	571.3	54.72	18.73	10.42	**7.14**	5.46	4.44	3.76	3.28
		DS	0.982	575.1	63.45	17.42	7.73	**4.56**	3.22	2.55	2.17	1.94
1.0		FP	1.00	273.2	53.83	18.99	9.19	5.41	3.64	2.69	2.14	1.79
	1.5	VSS	0.982	282.3	**21.77**	8.10	5.03	3.76	3.08	2.67	2.39	2.20
		EWMA	1.00	277.1	**20.40**[1]	9.24	6.03	4.53	3.66	3.10	2.71	2.42
		DS	0.997	273.84	**21.59**	6.16	3.23	2.29	1.87	1.63	1.48	1.37
	2.0	VSS	0.992	312.2	25.08	**6.62**	3.79	2.95	2.58	2.38	2.24	2.14
		EWMA	1.00	276.6	22.72	**8.77**	5.33	3.87	3.08	2.59	2.25	2.00
		DS	0.997	273.84	21.59	**6.16**[1]	3.23	2.29	1.87	1.63	1.48	1.37
	3.0	VSS	0.997	277.5	26.09	7.22	3.78	**2.74**	2.32	2.10	1.98	1.90
		EWMA	1.00	277.2	25.70	9.18	5.30	**3.75**	2.93	2.44	2.11	1.87
		DS	0.989	273.64	25.16	6.99	3.39	**2.23**[1]	1.75	1.50	1.36	1.26
1.5		FP	1.00	224.42	**36.54**	11.92	5.65	3.37	2.34	1.80	1.50	1.32
	1.5	VSS	0.999	231.57	**13.52**[1]	4.99	3.28	2.62	2.28	2.08	1.94	1.84
		EWMA	1.00	232.0	**14.88**	6.61	4.32	3.26	2.66	2.27	2.00	1.80
		DS	0.976	224.63	**14.16**	4.21	2.46	1.89	1.62	1.45	1.33	1.25
	2.0	VSS	0.979	224.53	15.50	**4.65**	2.88	2.34	2.12	2.01	1.94	1.90
		EWMA	1.00	229.3	16.43	**6.29**	3.86	2.84	2.29	1.94	1.71	1.54
		DS	0.976	224.63	14.16	**4.21**[1]	2.46	1.89	1.62	1.45	1.33	1.25
	3.0	VSS	0.998	234.80	18.20	5.03	2.87	**2.21**	1.93	1.76	1.64	1.55
		EWMA	1.00	224.6	17.31	6.36	3.81	**2.76**	2.21	1.87	1.64	1.47
		DS	0.981	228.00	18.05	4.90	2.44	**1.68**[1]	1.38	1.23	1.15	1.10
2.0		FP	1.00	220.6	29.84	9.04	4.20	2.54	1.82	1.46	1.26	1.15
	1.5	VSS	0.980	221.1	**10.20**[1]	4.28	3.04	2.53	2.26	2.09	1.95	1.85
		EWMA	1.00	221.5	**12.15**	5.46	3.60	2.75	2.26	1.95	1.72	1.56
		DS	0.999	221.79	**10.57**	3.24	2.02	1.59	1.37	1.24	1.16	1.11
	2.0	VSS	0.990	237.7	11.81	**3.67**	2.50	2.12	1.92	1.79	1.68	1.58
		EWMA	1.00	222.0	13.71	**5.12**	3.15	2.33	1.89	1.62	1.43	1.30
		DS	0.987	220.95	10.95	**3.27**[1]	1.99	1.57	1.35	1.23	1.15	1.10
	3.0	VSS	0.994	224.9	17.39	4.54	2.52	**1.93**	1.67	1.50	1.38	1.28
		EWMA	1.00	228.9	14.04	5.17	3.15	**2.33**	1.88	1.61	1.43	1.29
		DS	0.993	224.00	14.32	3.76	1.95	**1.42**[1]	1.21	1.12	1.07	1.04
3.0		FP	1.00	262.95	24.84	6.55	2.96	1.84	1.39	1.18	1.09	1.04
	1.5	VSS	0.992	270.27	**6.70**[1]	3.22	2.52	2.20	1.99	1.83	1.71	1.59
		EWMA	1.00	263.5	**9.85**	4.18	2.74	2.10	1.74	1.51	1.35	1.23
		DS	0.979	273.60	**7.76**	2.53	1.70	1.37	1.21	1.12	1.07	1.04
	2.0	VSS	0.994	265.83	8.04	**2.89**	2.19	1.92	1.75	1.61	1.49	1.39
		EWMA	1.00	263.1	10.50	**4.01**	2.54	1.92	1.58	1.37	1.23	1.14
		DS	0.984	263.44	8.56	**2.43**[1]	1.55	1.27	1.15	1.08	1.04	1.02
	3.0	VSS	0.996	271.91	17.88	3.81	2.11	**1.61**	1.37	1.23	1.13	1.07
		EWMA	1.00	267.3	10.66	4.03	2.54	**1.92**	1.58	1.37	1.23	1.14
		DS	0.995	268.62	11.67	2.82	1.52	**1.19**[1]	1.08	1.03	1.02	1.01
4.0		FP	1.00	352.14	23.46	5.43	2.40	1.53	1.21	1.08	1.03	1.01
	1.5	VSS	0.957	354.46	**5.87**[1]	2.98	2.41	2.16	2.01	1.90	1.82	1.74
		EWMA	1.00	355.1	**8.67**	3.80	2.55	1.98	1.65	1.44	1.28	1.17
		DS	0.988	358.65	**6.26**	2.14	1.52	1.27	1.15	1.08	1.04	1.02
	2.0	VSS	0.985	356.65	8.17	**2.56**	1.92	1.72	1.59	1.47	1.36	1.27
		EWMA	1.00	364.4	9.06	**3.56**	2.31	1.77	1.47	1.28	1.16	1.08
		DS	0.993	358.83	7.05	**2.00**[1]	1.36	1.16	1.07	1.03	1.01	1.01
	3.0	VSS	0.997	370.89	15.54	3.25	1.85	**1.44**	1.24	1.12	1.06	1.03
		EWMA	1.00	364.4	9.06	3.56	2.31	**1.77**	1.47	1.28	1.16	1.08
		DS	0.986	363.72	10.69	2.38	1.33	**1.10**[1]	1.03	1.01	1.00	1.00

_ Lowest ARL_1.

[1] Lowest ARL_1 in optimization point.

From Table 3 it is observed that in those scenarios where VSS-c or EWMA-c schemes were the best alternative to detect the critical shift, this condition of best option remains only for those shifts whose magnitude is very similar to that of the critical shift for which it was optimized ($\gamma \simeq \gamma^*$). Although, in most cases this condition is only retained at the optimization point ($\gamma = gamma^*$). On the other hand, the optimal DS-c scheme seems to be much more robust, since when it is best alternative to detect critical shift, this condition keeps it for all shift whose magnitude is greater than the critical shift ($\gamma \geq \gamma^*$). In addition, in those cases where DS-c is not the best option to detect the critical shift, it presents the best performance in almost the entire profile ARL_1. Especially for those shifts with moderate to large magnitude ($\gamma \geq 2.5$).

6 Conclusions

In this work we have made the optimal design proposal of a new double sample scheme for the control chart c (DS-c). Due to DS-c scheme having a greater number of parameters than its counterpart of fixed parameters (FP-c), its flexibility to meet a desired false alarm rate is much higher. This property is usually desired in the design of control graphics. Additionally, a bi-objective optimization procedure is presented, through which the practitioner can lead the design towards the optimization of one of two objectives, minimizing the average cost of the inspection process or minimizing the average time of detection of a shift. As a result of the procedure, the practitioner has a set of Pareto optimal solutions (Pareto front), from which he can select that which represents user trade off between both objectives (minimizing β or minimizing ASN). For example, from the Pareto front, the practitioner can select the solution that minimizes the inspection costs, guaranteeing the same efficiency of the c control chart in the detection of an increase in the average number of nonconformities. Alternatively, the user can select the solution that, guaranteeing the same inspection costs, optimizes the performance of the graph in detecting a change.

The performance of DS-c scheme was compared with the alternatives based on the variable sample size VSS-c and the EWMA-c. This comparison was made guaranteeing the equality of costs between the three schemes and the same frequency of false alarms. The results show that the performance of the DS-c scheme is only surpassed by one of the VSS-c and the EWMA-c schemes, when they have been optimized to detect a small increase in the average number of non-conformities ($\gamma^* = 1.5$) or when it is used for processes with very low number of nonconformities per inspection unit ($\lambda_0 = 0.5$). However, this loss of performance is only significant at the point of optimization. When the shift presented is greater than the critical shift ($\gamma > \gamma^*$) for which they were optimized, the DS-c scheme was always the best alternative.

References

Aparisi, F., Epprecht, E. K., and Mosquera, J. (2018). Statistical process control based on optimum gages. *Quality and Reliability Engineering International*, 34(1):2–14.

Aparisi, F. and Garcia-Diaz, J. C. (2004). Optimization of univariate and multivariate exponentially weighted moving-average control charts using genetic algorithms. *Computers & Operations Research*, 31(9):1437–1454.

Borror, C. M., Champ, C. W., and Rigdon, S. E. (1998). Poisson ewma control charts. *Journal of Quality Technology*, 30(4):352.

Chong, Z. L., Khoo, M. B., and Castagliola, P. (2014). Synthetic double sampling np control chart for attributes. *Computers & Industrial Engineering*, 75:157–169.

Chou, C.-Y., Wu, C.-C., and Chen, C.-H. (2006). Joint economic design of variable sampling intervals (x) and r charts using genetic algorithms. *Communications in Statistics—Simulation and Computation®*, 35(4):1027–1043.

Croasdale, R. (1974). Control charts for a double-sampling scheme based on average production run lengths. *International Journal of Production Research*, 12(5):585–592.

Daudin, J. (1992). Double sampling x charts. *Journal of quality technology*, 24(2):78–87.

De Araújo Rodrigues, A. A., Epprecht, E. K., and De Magalhaes, M. S. (2011). Double-sampling control charts for attributes. *Journal of Applied Statistics*, 38(1):87–112.

Deb, K., Pratap, A., Agarwal, S., and Meyarivan, T. (2002). A fast and elitist multiobjective genetic algorithm: Nsga-ii. *IEEE transactions on evolutionary computation*, 6(2):182–197.

Epprecht, E. and Costa, A. (2001). Adaptive sample size control charts for attributes. *Quality Engineering*, 13(3):465–473.

Epprecht, E. K., Costa, A. F., and Mendes, F. C. (2003). Adaptive control charts for attributes. *IIE Transactions*, 35(6):567–582.

Epprecht, E. K., Simões, B. F., and Mendes, F. C. (2010). A variable sampling interval ewma chart for attributes. *The International Journal of Advanced Manufacturing Technology*, 49(1):281–292.

He, D., Grigoryan, A., and Sigh, M. (2002). Design of double-and triple-sampling x-bar control charts using genetic algorithms. *International Journal of Production Research*, 40(6):1387–1404.

Holland, J. H. (1975). *Adaptation in natural and artificial systems: an introductory analysis with applications to biology, control, and artificial intelligence.* U Michigan Press.

Inghilleri, R., Lupo, T., and Passannanti, G. (2015). An effective double sampling scheme for the c control chart. *Quality and Reliability Engineering International*, 31(2):205–216.

Irianto, D. and Shinozaki, N. (1998). An optimal double sampling control chart. *International Journal of Industrial Engineering-Applications and Practice*, 5(3):226–234.

Mersmann, O., Trautmann, H., Steuer, D., Bischl, B., and Deb, K. (2014). Package "mco": multiple criteria optimization algorithms and related functions. *URL: https://cran. r-project. org/web/packages/mco/mco. pdf.*

Montgomery, D. C. (2009). *Introduction to statistical quality control*. John Wiley & Sons (New York).

Perez, E., Carrion, A., Jabaloyes, J., and Aparisi, F. (2010). Optimization of the new ds-u control chart: an application of genetic algorithms. In *Proceedings of the 9th WSEAS international conference on Applications of Computer Engineering*, pages 105–109.

Psarakis, S. (2015). Adaptive control charts: recent developments and extensions. *Quality and Reliability Engineering International*, 31(7):1265–1280.

Vaughan, T. S. (1992). Variable sampling interval np process control chart. *Communications in Statistics-Theory and Methods*, 22(1):147–167.

Whitley, D. (1994). A genetic algorithm tutorial. *Statistics and computing*, 4(2):65–85.

Wu, Z. and Luo, H. (2004). Optimal design of the adaptive sample size and sampling interval np control chart. *Quality and Reliability Engineering International*, 20(6):553–570.

Wu, Z. and Wang, Q. (2007). An np control chart using double inspections. *Journal of Applied Statistics*, 34(7):843–855.

Zitzler, E. and Thiele, L. (1999). Multiobjective evolutionary algorithms: a comparative case study and the strength pareto approach. *IEEE transactions on Evolutionary Computation*, 3(4):257–271.